Published in Proceedings of 2017 IEEE/RSJ International Conference on Intelligent Robots and Systems (IROS)
September 24–28, 2017, Vancouver, BC, Canada

Static Force Distribution and Orientation Control for a Rover with an Actively Articulated Suspension System

Florian Cordes[a], Ajish Babu[a], and Frank Kirchner[a,b]

***Abstract*— This paper presents the control strategies used to adapt the actively articulated suspension system of the rover SherpaTT to irregular terrain. Experimental validation of the approach with the physical system is conducted and presented. The coordinated control of the legs constituting the suspension system is encapsulated in a Ground Adaption Process (GAP) that operates independently from high level motion commands. The GAP makes use of force and orientation measurements to control the suspension system with 20 active degrees of freedom. The active suspension is used to achieve multi-objective terrain adaption encompassing (i) active force distribution at the wheel-ground contact points, (ii) keeping all wheels in permanent ground contact, and (iii) body orientation w.r.t. gravity.**

I. INTRODUCTION

Currently, planetary exploration is conducted exclusively by robotic means. Stationary landers with manipulators, scoops and remote sensing devices provide the possibility to collect information around a fixed landing site, one such example being the Phoenix lander on Mars [9].

A substantially larger area can be explored using mobile robots. For stable and robust locomotion an adaption to the irregular surface (dunes, slopes, boulders, soft soil, hard soil, etc.) is mandatory. Passive suspension systems allow an adaption to the ground with comparatively low complexity and little or no computational effort. Suspension systems as the triple bogie ExoMars suspension [6] or the well-known rocker-bogie suspension (as used for example in all four successfully deployed Mars rovers, [4, 5, 7]) are examples for passive suspensions providing a good terrain capability. In case of the rocker-bogie suspension, a differential reduces the angles experienced at the rover's body due to sloping terrain and climbing boulders. The size of obstacles that can be overcome is in the range of the wheel's diameter. To climb an obstacle with a wheel, the suspension system needs the other wheels to provide enough traction in order to push the wheel up the obstacle. Once stuck in soft soil or with a wheel in a crevice it might be hard for a system with passive suspension to free itself from that situation, as can be seen for example with the Spirit rover[1]. Furthermore, high peak rim thrusts that are far from the nominal thrust in regular operation have to be provided to drive a wheel vertically out of such a hole with up to half of the vehicle's weight on that wheel [12].

Fig. 1. SherpaTT in an artificial crater environment. Inset shows compact stow pose.

Current research is also directed towards active suspension systems for mobile robots. Active suspension has the potential to deliberately influence the robot's center of gravity, distribute forces between wheels, lift wheels off of the ground, or actively control the body's pose, e.g. roll and pitch w.r.t. a plane perpendicular to gravity. Hence, being more complex in general, an actively articulated suspension can yield substantially improved rough terrain mobility.

JPL's Sample Return Rover (SRR) is able to articulate its two shoulder joints in order to actively conform to sloping terrain [3]. By changing the suspension geometry, the position of the center of mass w.r.t. to the support polygon can be changed. In the experiments described in [3], the rover (1) drove a short traverse with a fixed suspension, and (2) stopped for adjustment of the suspension according to a planned sequence and then repeated (1)-(2) for the test track. A comparison of the stability margin with a fixed suspension showed a vast improvement with the articulated suspension.

The ATHLETE family of rovers [12] makes use of a fully actuated suspension without passive elements in the legs, apart from the flexible wheels. Each leg of a robot has six (seven in case of Tri-ATHLETE) active Degrees of Freedom (DoFs) to achieve active terrain adaption. Variances in absolute and relative position encoders are used to estimate the joint torques and an Inertial Measurement Unit (IMU) in the central body is used to measure the orientation of the central platform.

There are many more systems with active suspension to be found in the literature. An all-encompassing literature survey would be beyond the scope of this paper; [2] provides more literature concerning active and passive suspension systems.

*This work is part of the project TransTerrA and funded by the German Space Agency (DLR, Grant number: 50RA1301) with funds of the Federal Ministry of Economics and Technology (BMWi).

[a]DFKI Robotics Innovation Center Bremen, Bremen, Germany firstname.lastname@dfki.de

[b]University of Bremen, Faculty 03: Mathematics/Computer Science, Bremen, Germany

[1]http://mars.nasa.gov/mer/mission/status.html#spirit

This paper focuses on the rover SherpaTT, which is part of a multi-robot exploration system, built for and tested in an earth bound demonstration scenario [10]. Fig. 1 shows the rover in an artificial crater environment. The rationale for developing the active suspension system in SherpaTT is twofold: (i) the suspension design allows high terrain mobility for the rover, with active influence on the center of gravity's position in three dimensions, control of contact forces at wheel-ground contact points (load distribution), and orienting the main body irrespective of the terrain and (ii) the design allows the body to be moved with the wheels not changing their position on the ground. Hence, the system is able to deploy and pick up other compatible modules with its bottom electro-mechanical interface [10]. With the force sensors directly in the legs and an orientation measurement in the body, the complex system can be controlled with a minimal set of inputs. All leg movements for ground adaption can be done without the need to stop for reconfiguration of the legs. All controls demonstrated in this paper are based on these low-level sensors and a reactive control approach. Path planning for the system or suspension configuration planning is not needed for ground adaption and consequently not part of this work.

Controllers for actively articulated robots can be found in the literature. Wheeler in [11] develops a compliance model for wheel deflection to be used with walking gaits. In [8] Reid uses an RGB-D sensor to generate a terrain map and perform ground adaption using this information. In contrast to this high-level approach, in this paper, we discuss the solution with force measurement in each wheel and hence vastly simplified control, without relying on complex modeling and sensor processing.

II. MOTION CONTROL SYSTEM

This section gives an overview of SherpaTT's *Motion Control System (MCS)*. The DoF of the suspension system are described along with the general mechanical structure. Furthermore, the design of the ground adaption controller and insights of data processing such as the estimation of an ideal force distribution on the four ground contact points is provided.

A. Suspension System Kinematics

The suspension system consists of four leg-like structures with a wheel at the end of each leg. Each of the legs has five DoF in total, Fig. 2. Due to the design of the legs, a four dimensional workspace for each leg is achieved (3D position, 1D orientation). The robot is able to change its footprint from nearly six square meters (square with $2.4\,m \times 2.4\,m$ edge length) down to around one square meter in its *stow pose*, see also inset in Fig. 1.

The *Pan* joint rotates the leg around its pivot point on the central body. This allows changing the foot print from long stance to wide stance or a square stance, the latter being the standard configuration, also referred to as cross-stance [1]. The two joints, *InnerLeg* and *OuterLeg*, are designed as parallelograms to keep the wheel parallel to the rover's body.

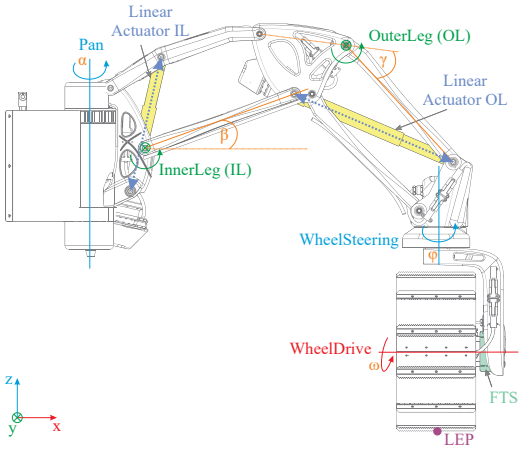

Fig. 2. Degrees of freedom of a suspension unit of SherpaTT, LEP, and location of the FTS.

Each parallelogram is equipped with a linear actuator. Using non-backdrivable linear spindle drives for actuation allows an energy-efficient self-locking, hence, the rover keeps its body height even when powered off. The *WheelSteering*-DoF is used for orienting the wheel while the *WheelDrive* actuator rotates the wheel to propel the robot and avoid wheel dragging during posture changes.

B. Overview of the Control Structure

An overview of the MCS is provided in Fig. 3. The control system has three main input classes, that can be used by human operators via a graphical user interface or from higher level processes (navigation, path follower and alike). The inputs encompass (i) a three dimensional motion command $\dot{\xi} = (\dot{x}, \dot{y}, \dot{\Theta})^T$ with velocities for forward, lateral and rotational movements of the robot, (ii) a footprint command consisting of four three dimensional vectors $\mathbf{g}_i$ ($i = \{0 \ldots 3\}$), defining the relative position of each Leg End Point (LEP) to the body, and (iii) a footprint-independent six-dimensional body posture $\mathbf{b} = (x_b\ y_b\ z_b\ \Omega\ \Phi\ \Psi)^T$.

The inputs are fed forward to a drive mode module, generating wheel orientation φ_i and wheel velocity ω_i commands from the motion command and a LEP command generator, that merges the body posture command with the footprint command to a single LEP command $\hat{\mathbf{p}}_i$ for each leg i.

The LEP command is then sent to an interpolation module in order to generate smooth trajectories between actual LEP ($\mathbf{p}_i$) and (newly) commanded LEP. The active *GAP* (see next subsection) writes z-offsets that are added to the interpolated LEP commands to be finally written (as $\bar{\mathbf{p}}_i$) via an inverse kinematics module to the hardware.

C. Active Ground Adaption: Overview

The GAP is composed of different submodules. Each contributes to the ground adaption of the suspension system by reacting to measured sensor values, as indicated within the orange box in Fig. 3. The GAP's submodules calculate individual offsets for each of the four legs that are added to the actual LEPs before the inverse kinematics layer generates the joint command $\bar{\mathbf{q}}_i$. The two key components of GAP are

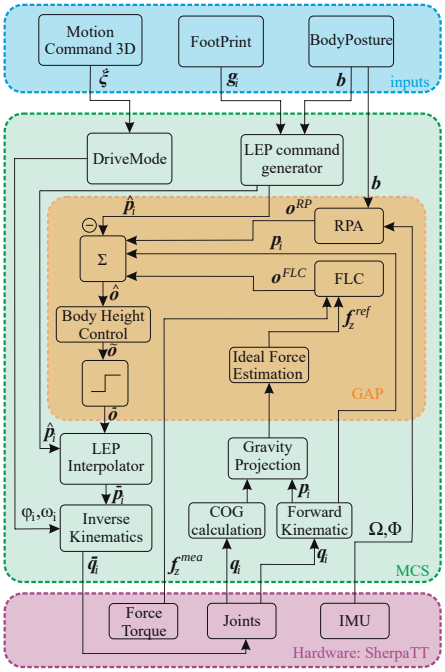

Fig. 3. Simplified structure of MCS with user/high-level inputs and details of the structure of the GAP (orange box)

the *Roll Pitch Adaption (RPA)* and *Force Leveling Control (FLC)* which ensure desired body orientation, and adequate wheel-ground contact, respectively.

The single offsets of RPA ($\mathbf{o}_i^{RP}$) and FLC ($\mathbf{o}_i^{FLC}$) are added in an accumulator module and then passed to the *Body Height Control* module that (i) removes common offsets from the legs (in case all accumulated offsets have the same sign), and (ii) limits the offsets such that the resulting LEP command is kept within the work space of a leg. By limiting the absolute offset outputs $\tilde{\mathbf{o}}$ in a saturation component, the final offsets $\bar{\mathbf{o}}$ for each leg are generated.

D. Force Leveling Control

The FLC component is implemented to maintain the expected force for each wheel in the current footprint, projected along the vector of gravity. The values measured from the force-torque sensors and the location of the Center of Gravity (CoG) within the support polygon are inputs to FLC. Note that the calculated "ideal" forces are those that are expected in the current foot print configuration of the robot, simply put, the closer the wheel to the body, the higher its load share. Ideal force distribution for locomotion improvement needs to change the location of the CoG within the support polygon. Driving up a slope, this might be achieved by shifting the robot's body upslope. Such a posture adaption is not the task of the FLC component.

The ideal forces are estimated under the assumption of static equilibrium with only the gravitational forces and their reaction forces from the ground acting on the robot. The static equilibrium assumption produces three constraint equations and four unknowns. This underdetermined system is solved using a Moore-Penrose pseudoinverse. By correcting each LEP's z-position with an offset o_i^{FLC} in order to match the measured forces with the expected forces, an optimal ground contact can be ensured for each LEP in the current posture of the robot.

For this goal, the LEPs and the CoG of the robot are projected onto a gravity perpendicular 2D plane using the IMU's attitude measurements. Let the position of the LEPs in the 2D plane be $\begin{pmatrix} x_i & y_i \end{pmatrix}^T$, with $i = \{0, 1, 2, 3\}$ representing each leg and the position of the CoG be $\begin{pmatrix} x_c & y_c \end{pmatrix}^T$. Let $\mathbf{t} = \begin{pmatrix} 0 & 0 & mg \end{pmatrix}^T$, be the vector consisting of zero-moments around x and y axis and gravitational force. Let the expected vertical reaction forces vector be $\mathbf{f}_z^{ref} = \begin{pmatrix} f_{z,0}^{ref} & f_{z,1}^{ref} & f_{z,2}^{ref} & f_{z,3}^{ref} \end{pmatrix}^T$ where $f_{z,i}^{ref}$ is the scalar value for each leg. The constraint equation for the static equilibrium case is given by

$$\mathbf{t} = \mathbf{A} \cdot \mathbf{f}_z^{ref} \tag{1}$$

where

$$\mathbf{A} = \begin{pmatrix} x_0 - x_c & x_1 - x_c & x_2 - x_c & x_3 - x_c \\ y_0 - y_c & y_1 - y_c & y_2 - y_c & y_3 - y_c \\ 1 & 1 & 1 & 1 \end{pmatrix} \tag{2}$$

Solving for $\mathbf{f}_z^{ref}$ yields

$$\mathbf{f}_z^{ref} = \mathbf{A}^+ \cdot \mathbf{t} \tag{3}$$

where $\mathbf{A}^+$ is the Moore-Penrose pseudoinverse for matrices with independent columns given by

$$\mathbf{A}^+ = \mathbf{A}^T \cdot (\mathbf{A} \cdot \mathbf{A}^T)^{-1} \tag{4}$$

$\mathbf{f}_z^{ref}$ is taken as reference input for FLC during each time step. The CoG is computed using the approximated inertial properties of the robot links. Inaccuracies in computation of CoG increase inaccuracy in the computation of ideal forces.

E. Roll-Pitch Adaption

The RPA component takes roll and pitch from the IMU data, and compares it against the desired roll Ω and pitch Φ for the body. The orientation error is computed in angle-axis form and used to compute the offsets o_i^{RP} necessary for roll-pitch correction. Let the orientation error be represented in angle-axis as $\{\mathbf{e}, \theta_e\}$, where $\mathbf{e}$ is the normalized rotation axis and θ_e is the rotation error in the Body Coordinate System. Since only roll and pitch errors are considered, $\mathbf{e}$ is always in the xy-plane. The desired offset for correcting the roll/pitch is dependent on the LEP's distance d_i to the rotation axis, while the sign is determined by the sign of θ_e and the LEP location $\mathbf{p_i} = \begin{pmatrix} p_{x,i} & p_{y,i} & 0 \end{pmatrix}^T$ in the xy-plane w.r.t. $\mathbf{e}$ ("left or right side").

$$o_i^{RP} = \pm\, d_i \tan\theta_e \tag{5}$$

$$d_i = \|\mathbf{e} \times \mathbf{p}\| \quad \text{because } \|\mathbf{e}\| = 1 \tag{6}$$

$$o_i^{RP} = \operatorname{sgn}(\mathbf{p} \cdot \mathbf{n})\, \|\mathbf{e} \times \mathbf{p}\|\, \tan\theta_e \tag{7}$$

where $\mathbf{n_i}$ the normal of the plane spanned by the rotation axis $\mathbf{e}$ and the basis vector along the robot's z-axis $\hat{k} = \begin{pmatrix} 0 & 0 & 1 \end{pmatrix}^T$.

F. Controller Implementation

The general approach for the active ground adaption is to keep the calculation efforts as low as possible for implementation on low performance hardware in future developments. Therefore an approach without sophisticated control-architecture, planning or exteroceptive sensors (e.g. laser scanner or camera) is chosen deliberately.

The FLC and RPA controllers are activated only if all the wheels are in contact with the ground, otherwise the legs which are not in contact are lowered until there is a minimal contact. The outputs from the FLC and RPA are position offsets for each leg in the vertical direction. The combined unsaturated offsets for each leg $\hat{o}_i$ are given by

$$\hat{o}_i = p_{z,i} - \hat{p}_{z,i} + K_f \cdot \left(f_{z,i}^{mea} - f_{z,i}^{ref} \right) + K_o \cdot o_i^{RP} \quad (8)$$

where K_f is the force-leveling gain, K_o is the orientation gain defining the overall influence of the modules on the GAP output. The values $\hat{\mathbf{o}} = (\hat{o}_0 \ \hat{o}_1 \ \hat{o}_2 \ \hat{o}_3)^T$ are then shifted by the body height control module and a saturation module as described in Section II-C to generate the final output value $\bar{\mathbf{o}}$.

The FLC module offset output is calculated as a scaled difference of measured force and reference force. The scaling is mainly done to transform the calculated scalar from force domain to distance domain. The effect is that of a simple proportional controller in velocity domain. In the experiments described below, the gains are hand-tuned, resulting in $K_f = 0.1 \frac{mm}{N}$ and $K_o = 1.0$.

The ability of the controller to overcome terrain height variations depends on the terrain slopes and on the robot speed. It is limited by the possible maximum speed of the leg movement, which in turn depends on the current leg configuration. The strategy is to linearly adapt the speed of the robot if the combined force and orientation errors crosses a predefined threshold. Experimental results in the regard are not included here.

III. EXPERIMENTS

All experiments presented are conducted in a laboratory environment with obstacles built up from modular components, Fig. 4. The experiments are conducted with a fixed commanded forward speed of $\dot{x} = 50 \frac{mm}{s}$. SherpaTT is in a symmetrical square-shaped footprint in all experiments with a commanded roll and pitch of zero degree for the body. The edge length of the foot print's square is about 2.1 m, i.e. when the front-left (FL) wheel is about to leave the obstacle which is 2.4 m in length, the rear-left (RL) wheel just entered the obstacle. The right side wheels roll over the even laboratory floor. The overall mass of the rover is about 150 kg in the experiments. With the symmetrical footprint, a symmetrical force distribution of $f_{z,i}^{ref} \approx 375\,N$ is to be expected. However, the manipulator's pose shifts the COG, imposing a slightly higher force on the front wheels. All experiments are conducted with rigid wheels. As shown in the image of the setup, the rover was in an early integration state for the experiments presented in this paper.

Fig. 4. Experimental setup (screenshot from experiment video). Overlay indicates dimensions of obstacle.

For reference, experiment markers are manually set in the data plots indicating the position of the wheels on the obstacle. The markers are shown in each of the following plots. A marker has the value zero, when the corresponding wheel is on the laboratory floor, the value one when the wheel is on an upward slope and the value two when the wheel is on a down slope of the obstacle. Preliminary tests showed only marginal deviations between single runs, hence the data shown here, even though from single runs, can be considered as relevant for the evaluation of the approach.

A. No Adaption: Rigid Suspension

A run without adaption is conducted as the baseline. The plots for the rover's roll and pitch angle and the z-forces at the four wheels are shown in Fig. 5(a) and Fig. 5(b), respectively. As expected, the forces strongly deviate from an ideal distribution throughout the run. While being on the obstacle, at least one wheel is without ground contact with $f_{z,i}^{ref} \approx 0\,N$.

As can be seen from the roll/pitch data, the rover tilts over its front-left/rear-right (FL/RR) axis at about 45 s during the run, effectively shifting the pitch angle to the roll angle. The touchdown of the front right wheel can be seen in a minimal force spike around the same time in the forces plot. The tip-over is the result of the slightly front-shifted COG due to the manipulator pose.

After starting the system and before entering the obstacle (≈5 s-25 s in the plot) the force distribution yields a *strong contact pair* (FL/RR) and a *weak contact pair* (front-right/rear-left; FR/RL). This can be explained by slightly different stiffness in the separate legs and minor inaccuracy in joint position calibration. During the run over the obstacle the strong contacts change from FL/RR to FR/RL when the rear wheel drives onto the obstacle. Slight deviations in leg stiffness and the preference for the FL/RR axis as strong contacts also explain, why at around 95 s there is a short period of ground contact of all four wheels (RL wheel is in "valley" between the two obstacle's peaks) while this is not the case around 45 s when the FL wheel is in that valley.

B. Using Roll/Pitch Adaption only

Fig. 6 shows the data when driving over the obstacle with active RPA and inactive FLC. At around 35 s the FL wheel is on the first top of the obstacle when the rover tips over (peak of 1.5deg in roll and pitch in the plot). While the wheel drives

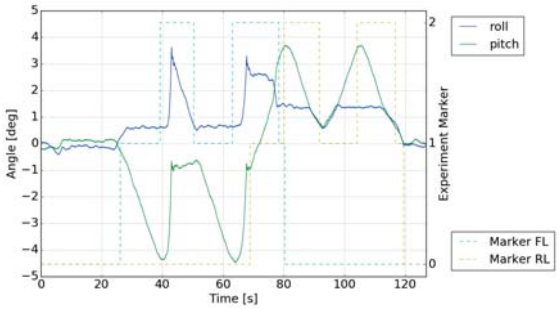

(a) Roll and pitch of body without any adaption

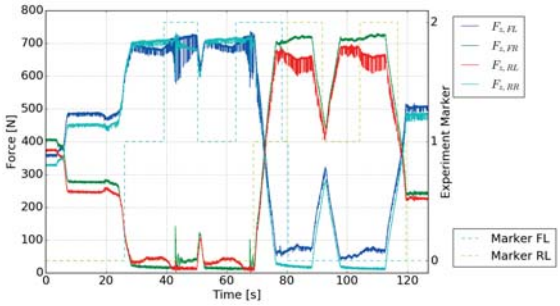

(b) Forces F_z on wheel contact points without any adaption

Fig. 5. Results from run without adaption, e.g. stiff suspension system

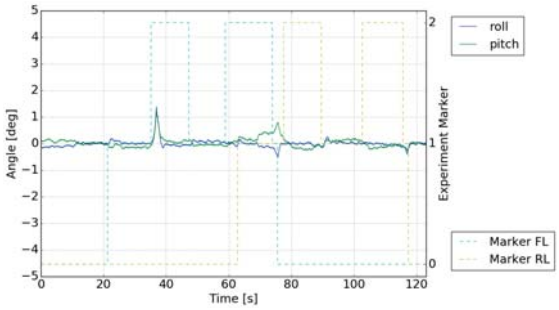

(a) Roll and pitch of body with RPA

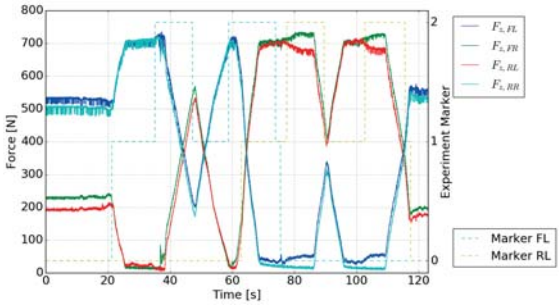

(b) Forces F_z on wheel contact points with RPA

Fig. 6. Results from run with RPA only. As expected the forces are similar to rigid suspension, while roll and pitch errors are clearly reduced.

down the slope, the forces at FL and RR decrease resulting in a short switch over of the strong contact axis.

Since the RPA module itself does not guarantee ground contact, contact loss is still observable. Even more: When entering the obstacle with the FL wheel, both, FL and FR wheels are moved up synchronously in order to reach the desired pitch, hence the FR wheel is moved up by the RPA module, when it actually should move down to keep ground contact. Apart from the roll/pitch deviations due to tipping over (at around 35 s onto FR wheel and at around 75 s onto FL wheel), the RPA module keeps both angles well within $\pm 0.5°$ with a commanded angle of zero degree, whereas deviations of $-4.5°$ to $+3.5°$ are present in the reference experiment without active adaption.

C. Using Force Leveling only

The experiments with FLC active and RPA inactive showed that the FLC has the tendency to impose a drift on the pitch angle of the robot. This is due to inaccuracies in the modelled weights of each of the links of the robot and the resulting inaccuracy in the position of the robot's COG. Due to this drift, these experiments are not presented in detail in this paper. The FLC alone in its implementation state while conducting the experiments discussed here is not feasible for usage in the active ground adaption.

D. Using Roll/Pitch Adaption and Active Force Leveling

In this experiment, the rover is commanded to keep the body's roll and pitch at zero degrees and simultaneously maintaining each wheel's desired z-force. Keeping the force at each wheel at the commanded value also ensures that the wheels do not loose ground contact. Due to the continuous ground contact of all wheels, no tip-over of the system occurs. Thus the roll and pitch angles are limited within $\pm 0.5°$ during the whole run, as shown in Fig. 7(a).

The forces at each wheel are displayed in Fig. 7(b). A clear improvement in distribution of the robot's weight onto all four wheels can be seen. After activating the FLC component (around 5 s in the plot), the forces are kept permanently between 250 N and 450 N (peaks around 15 s, 55 s, 60 s, and 110 s where wheels are entering or leaving the obstacle) and between 320 N and 400 N most of the time.

IV. CONCLUSION & OUTLOOK

The design of the presented Ground Adaption Process within SherpaTT's Motion Control System with modules for orientation adaption and force leveling provides an effective, yet simple-to-implement controller.

The experiments conducted and presented in this paper show a clear improvement from using no active adaption over only body orientation control to the combination of two adaption modules for achieving a multi-objective ground adaption. Fig. 8 shows the RMS errors from the three experiment settings. Roll/pitch control improvement is observable with the RPA active, reducing the RMS from 1.19° and 2.07° to values below 0.25°. The mean force error is lower (from 265 N to 253 N) but shows no significant improvement in this setting. Enabling FLC and RPA shows a greatly reduced force error (average error is 39 N) and reduces the roll error slightly in comparison with RPA only. The pitch error seems not to be influenced by activating the FLC.

While writing this paper, the system SherpaTT successfully finished a four week field deployment in the desert

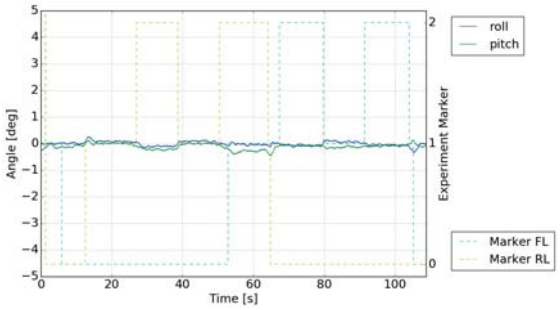

(a) Roll and pitch of body with RPA and FLC

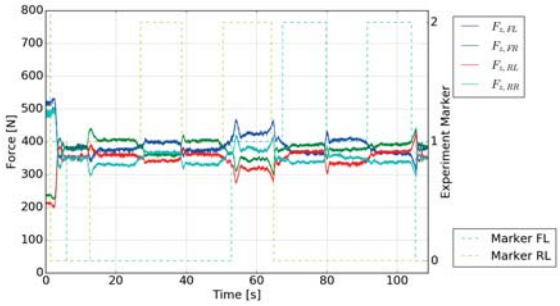

(b) Forces F_z on wheel contact points with RPA and FLC

Fig. 7. Results from run with RPA and FLC active. Both, forces at LEPs and roll/pitch error benefit from active FLC.

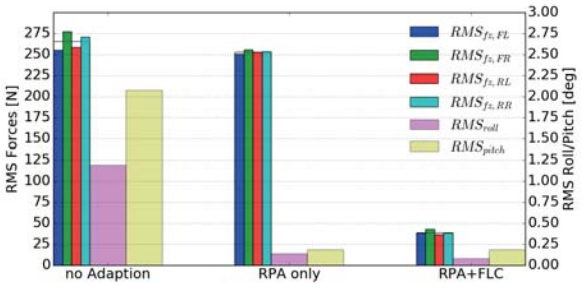

Fig. 8. RMS error of the three experiment settings. Average of force error of the four LEPs is displayed as underlying rectangle.

of Utah, USA[2] using the control approaches presented in this paper. The system was able to climb slopes of up to 28° covered with loose soil and duricrust. The data of these trials is currently being analyzed and will be published accordingly. Fig. 9 shows the system during a slope run on natural terrain.

Fig. 9. SherpaTT during field trials in Utah, USA in Oct/Nov 2016. Slope in this image is about 28°/53% and covered with duricrust. SherpaTT uses FLC and RPA modules to climb the slope.

References

[1] F. Cordes, A. Dettmann, and F. Kirchner. "Locomotion Modes for a Hybrid Wheeled-Leg Planetary Rover". In: *Proceedings of the IEEE International Conference on Robotics and Biomemetics (IEEE-Robio 2011)*. Phuket, Thailand, Sept. 2011.

[2] F. Cordes et al. "An Active Suspension System for a Planetary Rover". In: *Proceedings of the International Symposium on Artificial Intelligence, Robotics and Automation in Space (i-SAIRAS 2014)*. Montreal, Canada: o.A., June 2014.

[3] Karl Iagnemma and Steven Dubowsky. *Mobile Robots in Rough Terrain – Estimation, Motion Planning, and Control with Application to Planetary Rovers*. Vol. 12. Springer Tracts in Advanced Robotics 1. Springer-Verlag Berlin Heidelberg, 2004.

[4] NASA JPL. *Wheels and Legs*. http://mars.nasa.gov/msl/mission/rover/wheelslegs/. 2017-01-24.

[5] R.A. Lindemann and C.J. Voorhees. "Mars Exploration Rover mobility assembly design, test and performance". In: *Systems, Man and Cybernetics, 2005 IEEE International Conference on*. Vol. 1. Oct. 2005, 450–455 Vol. 1.

[6] S. Michaud et al. "ExoMars Locomotion Subsystem Analytical Tool Development and Correlation". In: *11th Symposium on Advanced Space Technologies in Robotics and Automation, ASTRA-11*. 2011.

[7] A.H. Mishkin et al. "Experiences with operations and autonomy of the Mars Pathfinder Microrover". In: *Aerospace Conference, 1998 IEEE*. Vol. 2. Mar. 1998, 337–351 vol.2.

[8] William Reid et al. "Actively articulated suspension for a wheel-on-leg rover operating on a Martian analog surface". In: *Robotics and Automation (ICRA), 2016 IEEE International Conference on*. IEEE. 2016, pp. 5596–5602.

[9] P.H. Smith. "The Phoenix mission to Mars". In: *Aerospace Conference, 2004. Proceedings. 2004 IEEE*. Vol. 1. Mar. 2004, 342 Vol.1.

[10] R. Sonsalla et al. "Towards a Heterogeneous Modular Robotic Team in a Logistic Chain for Extraterrestrial Exploration". In: *Proceedings of the International Symposium on Artificial Intelligence, Robotics and Automation in Space (i-SAIRAS 2014); June 17-19, Montreal, Canada*. o.A., June 2014.

[11] D. Wheeler, D. Chavez-Clemente, and V. SunSpiral. "FootSpring: A Compliance Model for the ATHLETE Family of Robots". In: *Proceedings of the 10th International Symposium on Artificial Intelligence, Robotics and Automation in Space (iSAIRAS'10)*. 2010, pp. 644–651.

[12] B. H. Wilcox. "ATHLETE: A limbed vehicle for solar system exploration". In: *2012 IEEE Aerospace Conference*. 2012, pp. 1–9.

[2]Video available at: `https://youtu.be/pvKIzldni68`